Tyre model development using co-simulation technique for helicopter ground operation

Wang, Y. , Blundell, M. V. , Woodand, G. and Bastien, C. J.

Tyre Model Development Using Co-Simulation Technique for Helicopter Ground Operation

Yun Wang, M V Blundell, G Wood and **C Bastien**

Vehicle Dynamics and Safety Applied Research Group, Coventry University, UK.

Abstract

This paper describes the development of a new aircraft tyre model applied using a co-simulation approach for the multibody dynamic simulation of helicopter ground vehicle dynamics. The new tyre model is presented using a point follower approach that makes a novel contribution to this area by uniquely combining elements of two existing tyre models used by the aircraft industry, namely the NASA R64 model developed by Smiley and Horne [1] and the ESDU (Engineering Sciences Data Unit) Mitchell tyre model [2].

Before the tyre model was used with a full helicopter model, a virtual tyre test rig was used to examine the tyre and to predict the tyre forces and moments for a range of tyre states. The paper concludes by describing the successful application of the new tyre model with a full helicopter model and the simulation of representative landing, take-off and runway taxiing manoeuvres. The predictive capability of the model is demonstrated to show the open-loop ground vehicle dynamics response of the helicopter and also the ground load predictive capability for the distribution of loads through the tyres, wheels and landing gears.

Mechanical, Automotive and Manufacturing Engineering Department, Coventry University, UK

Corresponding Author:
Yun Wang, Mechanical, Automotive and Manufacturing Engineering Department, Coventry University, Priory Street, Coventry, CV1 5FB, UK
Email: wangy21@uni.coventry.ac.uk

Nomenclature

A_1, A_2 – vertical force coefficient

B_1 to B_5 – cornering power coefficients

C_1, C_2 – tyre yaw angle parameter

C_z – coefficient in expression for tyre deflection under normal load

C_c – coefficient in expression for N

D – tyre diameter

D_1 – lateral force coefficient

E_1 to E_4 – aligning moment coefficients

h – half length of tyre ground contact area

N – cornering power

n – user define coefficient

p – tyre pressure

p_r – rated tyre pressure

R_u – unloaded radius

R_l – actual radius $\qquad R_l = R_u + \delta$

R_e – effective radius

w – width of the tyre

W_z – steering angle

Z – normal load

δ – tyre vertical deflection

σ – relaxation length

Φ – tyre yaw-angle parameter

Ψ_{tyre} – tyre yaw (or slip) angle

λ_0 – lateral distortion at the wheel centre

λ_1 – lateral distortion one step before the contact patch centre

λ_2 – lateral distortion one step after the contact patch centre

μ_Ψ – coefficient of friction

$\mu_{\Psi\,max}$ – maximum attainable value of force or friction coefficient in unbraked yawed rolling and in braked unyawed rolling

μ_r – ratio between $\mu_{\Psi\,max}$ and dry road friction coefficient

1. Introduction

In helicopter design, multibody dynamics software is used to simulate helicopter landing simulations either on the ground or on a ship's flight deck where the interaction between the tyre and landing surface has historically been modelled with contact forces. Helicopters are, however, often required to taxi at speed across runways where the potential to interact with disturbances may introduce vibration in the landing gears or in the worst case result in wheel shimmy. Problems in this area which are not identified at the design stage may lead to operational speed restrictions and degrade operational performance in critical situations.

Over the past fifty years, many mathematical models of the pneumatic tyre have been developed primarily for automotive applications but also for fixed wing aircraft. Very little however, has been undertaken in this area specifically for helicopters. Tyre properties play a crucial role in the predictive simulation of ground vehicle dynamics. Apart from aerodynamics forces the forces and moments generated in the tyre contact patch provide the main control for the aircraft while on the ground.

Early work in the automotive area required that a tyre existed and was tested using a tyre test machine before a computer simulation could be performed. The very early tyre models often used an interpolation approach, simply representing the test data as arrays that could be interpolated during the simulation. Although this captured the performance of the tyre these models were not parameter based and had no value as a design tool to investigate the sensitivities of the vehicle response to parameters such as tyre cornering stiffness.

For automotive handling studies, the tyre model that is now most well established is based on the work by Pacejka and is referred to as the "Magic Formula" (MF) [3]. The Magic Formula is not a predictive tyre model but is used to empirically

represent previously measured tyre force and moment curves. The first version developed is sometimes referred to as the "Monte Carlo version" due to the conference location at which this model was presented in the 1989 paper.

The Magic Formula model is undergoing continual development, which is reflected in a further publication where the model is not restricted to small values of slip angle and the wheel may also run backwards. The authors also discuss a relatively simple model for longitudinal and lateral transient responses restricted to relatively low time and path frequencies. The tyre model in this paper also acquired a new name and was referred to as the 'Delft Tyre 97' version, which has reverted over time to MF-Tyre 5.0. Also the "Delft-Tyre" model has become an umbrella term to include not only the base MF-Tyre model but a modified version of it suitable for intermediate frequency events known   [4].

Although the Magic Formula is widely used in the automotive and aircraft sector (including helicopters), its capability is constantly face against different range of challenges. Aircraft taxiing manoeuvres can lead to much larger slip angles (also referred to as yaw angles) than those on automotive vehicles. While car tyres may typically operate with slip angles of less than 10 degrees, even during severe manoeuvres, for this particular investigation the helicopter tyres were subject to slip angles up to 90 degrees. It is important to predict the carcass elasticity and transient behaviour in manoeuvres such as cornering, braking and taxiing. Aircraft and helicopters also often use bias tyres rather than the radial tyres established in the automotive sector. In general the main problem in aerospace applications is the absence of large scale tyre test programmes and a resulting lack of tyre test data. This renders models such as the MF tyre model, although proven to be accurate, difficult to use due to the large model parameter sets and the amount of experimental data required to populate these. The aim of this project was therefore to develop a tyre model with relatively low data input requirements. However, the model still needed to capture most of the tyre dynamic behaviour and to be compatible with a range of simulation scenarios.

The tyre model developed in this project was tested using a virtual tyre test rig model developed in a multibody systems environment in order to support the

theoretical development of the model. Trial data sets were used to produce typical graphs of tyre forces and moments as a function of vertical force and slip angle. Finally a full scale helicopter model was developed and used to successfully demonstrate the ground dynamics of the helicopter and the load prediction capability for landing, takeoff and taxiing manoeuvres.

2. Review of Existing Tyre Models

Over the past fifty years, several approaches have been taken to develop mathematical models to predict tyre behaviour. The tyre properties play a crucial role when determining vehicle dynamic behaviour, due to the fact that tyres are the only component which makes contact with the ground and provide the most significant input to control vehicle motion and trajectory. There are in the main three different categories of tyre models:

Analytical Models: the modelling of tyre/road contact was developed before the 1980s and mainly involves a point contact method, rigid tread band model and fixed footprint model. Despite this, some of these models can only achieve relatively low accuracy. However, they provided fundamental knowledge of the principal characteristics of the tyre and contribute to the analytical components of a terrain-vehicle interaction model used for dynamic vehicle simulation. These models include:

    Brush Models - These models are based on a relatively simple representation of the tyre structure where the model assumes the tyre to behave like an elastic element. The tyre tread is represented by an array of small elastic rectangular elements attached to a rigid ring. Each of the small elements possesses mass and captures the transient effects introduced by the previous element as they enter in and out of the contact patch [5]. This model has also been expanded upon by Mavros [6] where the model includes viscoelastic circumferential connections between the sequential bristles introducing a lateral degree of freedom. The instantaneous state of the bristle depends on the state of the same bristle at the preceding time step, as well as on the state of the two adjacent bristles at the same time. A comparison was undertaken between the simple and expanded version of

the brush model and the results showed that the extended version can capture certain oscillations such as the tyre transition from elastic deformation to the slipping phase.

Gim and Nikravesh [7-9] have also conducted a detailed study for the development of an analytical model of a pneumatic tyre. The first part of the study included a brief review on tyre characteristics along with several algorithms for computational modelling purposes. The second part of the study focused on an analytical approach for determining tyre dynamic properties. The equations derived in these papers describe a mathematical model for calculating the principle forces and moments of a tyre. For the final part of the study the analytical formulations were derived for the tyre dynamic properties as a function of the slip ratio, slip angle, camber angle and other tyre dynamic parameters. These formulations can be used for the general vehicle simulations in different terrain conditions. The tyre model results were also compared with experimental results. The analytical predictions of the longitudinal and lateral forces show good agreement with the experimental values.

Harty Model - This model was developed to increase the accuracy and potential of a low parameter tyre model. The model is similar in structure to the Fiala tyre model, but has been significantly developed by incorporating new methods to eliminate the major limitations in the Fiala tyre model. Improvements have been made to the longitudinal and lateral force calculations along with better curve fitting methods that have been utilised by introducing a series of scale factors [10].

Semi-Empirical/Empirical Models: In order to improve the accuracy problem caused by simplification in analytical modelling, semi-empirical/empirical models have been developed. These models are developed using experimental data; the formulation compensates for the margin of error introduced by theoretical assumptions in analytical methods. Several classical empirical models have been developed and are still being used for current tyre dynamic analysis.

Magic Formula - This is a widely used tyre model which permits the calculation of the tyre forces and moments in various conditions. In Pacejka's early research, several types of mathematical functions were used to represent the cornering force characteristics. Different equations such as exponential, arctangent, parabolic and hyperbolic tangent functions were investigated to successfully model the tyre dynamic characteristics. There are several versions of the Magic Formula in which its use is extended to combined longitudinal, lateral slip and camber angle within a simulation. The equations derived include a number of micro-coefficients which have to be determined from experimental data. The model provides simulation results that better fit the measured data. The Magic Formula tyre model has wide spread use today and is constantly evolving [3]. The model was further expanded to adopt higher frequency response and this version is called the SWIFT (Short Wavelength Intermediate Frequency Tyre) tyre model. The SWIFT tyre model is based upon the Magic Formula. The SWIFT tyre model is able to describe dynamic tyre behaviour for in-plane (longitudinal and vertical) and out-of-plane (lateral, camber and steering) motions up to about 60Hz, whilst also being able to accommodate road obstacles with short wavelength. Due to accuracy and calculation speed the SWIFT model has been programmed as a semi-empirical model which is derived using advanced physical models and a dedicated high frequency tyre measurement to assess the speed effects in tyre behaviour [4].

FTire Model - The FTire model is a flexible ring tyre model developed by Gipser [11]. It is a full 3D nonlinear in-plane and out-of plane tyre simulation model. It is designed for vehicle comfort simulations and prediction of road loads on road irregularities even with extremely short wave-lengths. It can also be used as a structural dynamics base to investigate highly non-linear and dynamic tyre models for handling studies without limitations or modification to its input parameters.

Finite Element Tyre Models: Over the past twenty years numerical analysis, especially finite element analysis (FEA), has been increasingly applied during the tyre design process. This method is time consuming but is potentially more accurate and applicable for tyre simulation [12].

It can be seen that tyre models are developed for a specific purpose. Different levels of accuracy and complexity may be introduced in each approach. Current empirical tyre models used by the automotive industry are very advanced and widely used for vehicle handling manoeuvres but are not directly applicable to helicopter tyres due to the lack of suitable test data. Currently the commissioning of an extensive range of tyre testing to develop helicopter tyre model data is not feasible. The purpose of this study was therefore to review existing automotive and aircraft tyre models and to develop a new tyre model specifically for helicopter ground simulations.

3. Tyre Modelling

There are two significant approaches for the modelling of a tyre which will be discussed in this section. Between 1950 and 1952 Moreland [13] developed a tyre model specifically for shimmy investigations. Moreland treated the tyre surface as small grids connected together to represent the tyre surface rolling into the contact patch and the influence of the road surface. The second method was the 'string' method developed by Von Schlippe [3], which treated the tyre as a section of string which deforms and returns back to its original shape as the tyre rolls in and out of the contact patch. In addition to Moreland's theories the work of Smiley and Horne [1] is also widely recognised.

The purpose of creating a tyre model is to predict the forces and moments acting through the tyres when the vehicle is traversing different road or terrain conditions, these being the forces, longitudinal force (F_x), lateral force (F_y) and vertical force (F_z) and the moments, overturning moment (M_x), rolling resistance moment (M_y) and aligning moment (M_z). Previous researchers such as Moore [14], Grossman [15] and Haney [16] have developed sophisticate methods of estimating tyre forces and moments for tyre modelling and aircraft landing gear investigations. Further to this, research has been undertaken by Butts and Kogan [17] looking at investigating helicopter landing gear shimmy using the UA-Tire model (a tyre model develop by University of Arizona).

Sophisticated automotive tyre models can require a high number of tyre model parameters and extensive data on which these can be based. The tyre data for aircraft modelling is very limited due to the cost and limited testing facilities. The tyre data provided for this investigation was limited and as such, the new tyre model for this investigation needed to have relatively low data input requirements. Considering the practicality and available of tyre data for model development, the author decided to begin development of the tyre model using the model from Mitchell [2] as a base due to the availability of data for this model from the project partner. For the tyre model development, equations were extracted from Mitchell [2] and Blundell and Harty [18] to model the lateral force, aligning moment, longitudinal force, rolling resistance moment and aligning moment. However, Mitchell [2] only provided equations for the vertical force, lateral force and aligning moment. There was no information on the overturning moment or tyre lateral distortion. To accommodate this several equations were adopted from the work of Smiley [19] and the R-64 model by Smiley and Horne [1]. A summary is provided in Table 1 to show the work of previous authors that informed the development of the model force and moment components in this study.

	Tyre model and equations used
Longitudinal force (F$_x$)	Free Rolling – Blundell [18] (Braked – Balkwill [20])
Lateral force (F$_y$)	ESDU model Mitchell [2]
Vertical force (F$_z$)	ESDU model Mitchell [2]
Overturning Moment (M$_x$)	R-64 Smiley [1 & 19] and Blundell and Harty [18]
Rolling Resistance Moment (M$_y$)	Blundell and Harty [18]
Aligning Moment (M$_z$)	ESDU model Mitchell [2]

Table- 1 Tyre models and equations used for tyre model development

With the combination of different models, the new model only required twenty three model input parameters. Details of the formulations and equations used with the new model are described in the following sections.

3.1 Vertical Load

As the tyres are the only components that make contact with the ground, road inputs and landing operations will introduce vertical force inputs to the tyres causing them to deform and transfer load to the vehicle structure [2]:

$$\frac{\delta}{w} = C_z + \frac{Z}{A_1(p + A_2 P_r)w(wD)^n} \tag{1}$$

Equation 1 gives a method of calculating the tyre deflection. The coefficient Cz varies with different aircraft tyres, for modern cross-ply tyres, the value is 0.03.
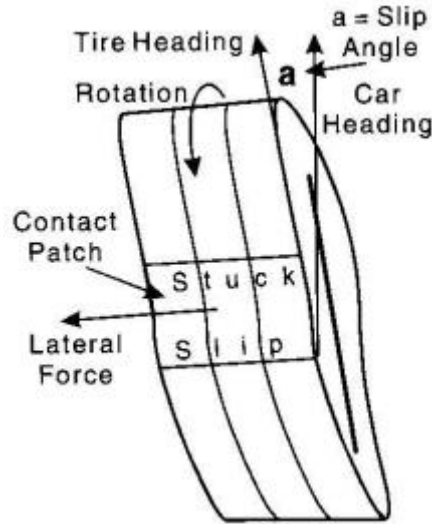
Figure- 1 Contact patch under slip angle [16]

The contact patch is the portion of a tyre that is in actual contact with the road surface. In Figure- 1 the 'stuck slip' area is in contact with the ground and the tyre is distorted due to the slip angle. For tyre dynamic studies, half the contact patch length [2] is calculated by the following equation:

$$\frac{2h}{D} = 1.7 \left[\frac{\delta}{D} - \left(\frac{\delta}{D} \right)^2 \right]^{0.5} \tag{2}$$

3.2 Cornering Power

The equations (3) and (4) were extracted from [2] which provided a method of estimating the cornering power (N) as a function of tyre geometry, deflection and inflation pressure. The two equations are governed by the ratio between the tyre deflection and tyre diameter. If the ratio is lower than 0.0875 then equation 3 becomes true; if the ratio is larger than 0.0875 the equation 4 becomes true. The coefficient (C_c) varies with tyre age and condition. For modern high-pressure tyres the coefficient is 1, for low-pressure tyres the coefficient is approximately 1.2 and for older tyres the coefficient is taken as 1.1.

$$\frac{N}{C_c(p + B_1 p_r)w^2} = B_2\tau - B_3\tau^2 \quad for\ \tau < 0.0875 \tag{3}$$

$$\frac{N}{C_c(p + B_1 p_r)w^2} = B_4 - B_5\tau \quad for\ \tau > 0.0875 \tag{4}$$

9

3.3 Tyre Yaw-Angle Parameter

Mitchell's model has a unique parameter called the tyre yaw-angle parameter [2]. This is the ratio between the cornering power and the normal load taking into account the coefficient of friction. This parameter is not only utilised in the lateral force and aligning moment calculation, but it is also used to determine whether the tyre is in the linear deformation state or slipping state.

$$\Phi = \frac{N \times \Psi_{tyre}}{Z[\mu_\Psi]_{max}[C_1 + C_2\mu_r]} \tag{5}$$

3.4 Lateral Force Calculation

Equations (6) and (7) illustrate a method for calculating the lateral force where the equation is governed by an absolute value of the tyre yaw-angle parameter (Φ) [2]. For cases when the absolute tyre yaw-angle parameter is smaller than 1.5, equation 6 is used. If the absolute tyre yaw-angle parameter is larger than 1.5, equation 7 is used to predict the lateral force.

$$\frac{F_y}{Zh[\mu_\Psi]_{max}} = \Phi - D_1\Phi^3 \quad for \ |\Phi| < 1.5 \tag{6}$$

$$F_y = Z \times [\mu_\Psi]_{max} \quad for \ |\Phi| > 1.5 \tag{7}$$

3.5 Self-aligning Moment

Mitchell utilises three equations (8-10) for the aligning moment and pneumatic trail calculation in order to improve accuracy [2]. The number of tyre parameters required for this model is still relatively low. However, the more advance curve fitting method utilised in the aligning moment has significantly improved the accuracy of the model.

$$\frac{M_z}{Zh[\mu_\Psi]_{max}} = E_1\Phi \quad for \ |\Phi| < 0.1 \tag{8}$$

$$\frac{M_z}{Zh[\mu_\Psi]_{max}} = \Phi - |\Phi|\Phi - E_2\frac{|\Phi|}{\Phi} \quad for \ 0.1 < |\Phi| < 0.7 \tag{9}$$

$$\frac{M_z}{Zh[\mu\psi]_{max}} = E_3 \frac{|\Phi|}{\Phi} - E_4\Phi \ for \ 0.7 < |\Phi| < 1.2 \tag{10}$$

3.6 Rolling Resistance Moment and Longitudinal Force

Rolling resistance is due to the energy losses in the tread rubber and side walls as sections of the tyre roll through the tyre contact patch. One of the causes of energy loss in the tyre is hysteresis. A block of rubber or tyre material requires more force to cause displacement during the loading phase than the unloading phase. As tyre material moves through the contact patch, it will be loaded until it reaches the midpoint of the contact patch and unloaded as it moves to the rear of the contact patch. This results in a pressure distribution that is not symmetric with higher pressure in the front half of the contact patch as show in Figure-2.
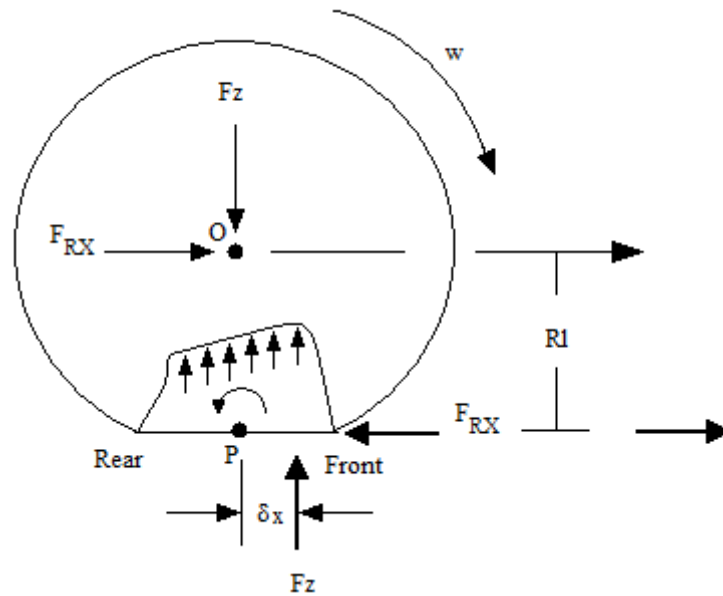

Figure- 2 Generation of rolling resistance in a free rolling Tyre [18]

The pressure distribution results in the vertical tyre force F_z acting a distance δ_x forward from the wheel centre. For equilibrium a couple exists that must oppose the tyre load and its reaction acting down through the wheel centre. The couple that reacts the wheel load couple results from the rolling resistance force F_{RX} acting longitudinally at the contact patch in a direction opposing travel:

$$F_{RX} = \frac{F_z \delta_x}{R_l} \tag{11}$$

Equation (11) applies for a free rolling tyre [18]. Although the tyres on a helicopter are not subject to tractive driving forces, during braking a set of equations, as defined by Balkwill [20] and Page [21], is used to calculate the longitudinal force.

The rolling resistance moment M_y is calculated using [18]:

$$M_y = F_z \delta_x \tag{12}$$

The rolling resistance moment may be further expanded to incorporate a rolling resistance coefficient (this being the rolling resistance force F_{Rx} divided by the tyre load F_z). By definition the rolling resistance moment, M_y, is $F_z \delta_x$ and therefore the rolling resistance moment coefficient is δ_x.

The rolling resistance force is very small in comparison with the other forces acting at the contact patch. A rolling resistance coefficient of 0.01 is typically used for a car tyre. This coupled with the fact that rolling resistance force may vary up to 30% from the average value during one revolution [18] makes accurate measurement difficult.
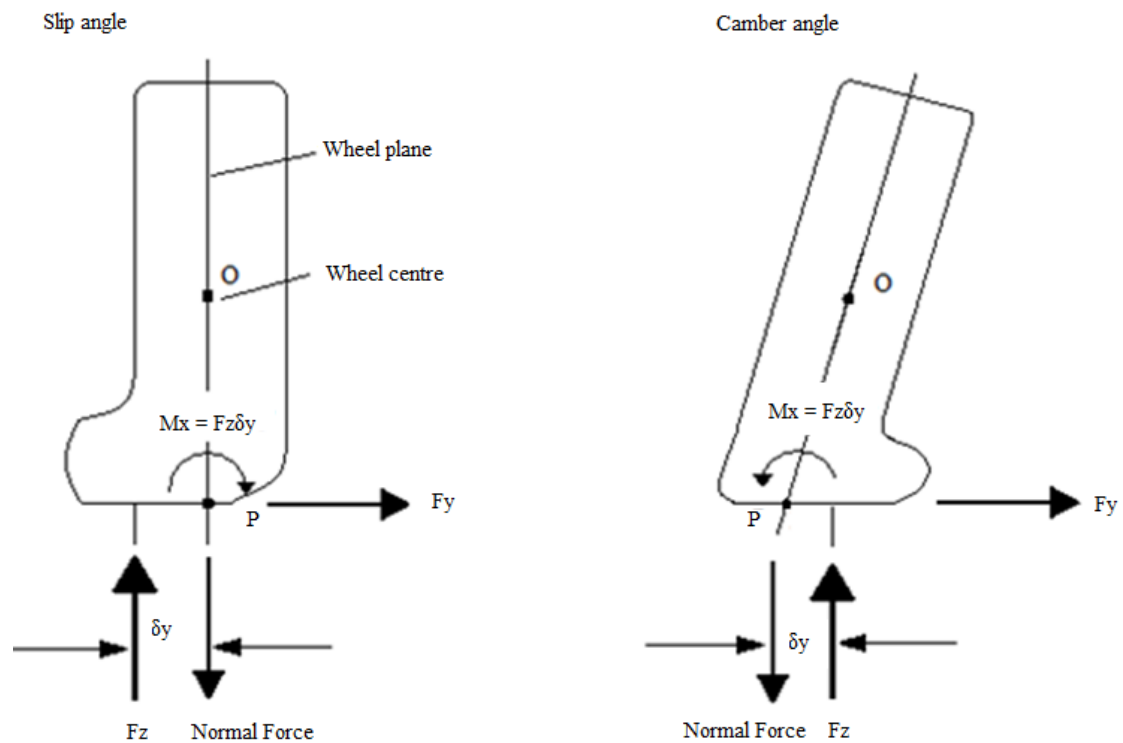
3.7 Overturning Moment

Figure- 3 Generation of overturning moment in the tyre contact patch [18]

The generation of lateral force due to slip angle, camber angle or a combination of the two can cause lateral distortion of the side walls resulting in a lateral shift of the contact patch. The resulting offset in tyre load introduces an additional moment M_x. In Figure- 3, F_z is represented as the tyre load acting on the tyre rather than the negative normal force. The lateral distortion (δ_y) on the left in Figure- 3 represents the lateral distortion caused by slip angle. The lateral distortion (δ_y) on the right of Figure- 3 represents the lateral distortion caused by camber angle. The two moments act in opposite directions and overturning moment becomes important where relatively large lateral displacements occur in the aircraft tyres [19]. The lateral distortion δ_y caused by camber angle can be calculated using the vertical displacement between the wheel centre and the ground together with the inclination angle. The lateral distortion δ_y caused by slip angle can be calculated by adopting several equations from Smiley [1,19] and Blundell and Harty [18]. The parameters, such as contact patch length and relaxation length, required to obtain the lateral distortion caused by slip angle are described in the following section.

3.8 Lateral Distortion
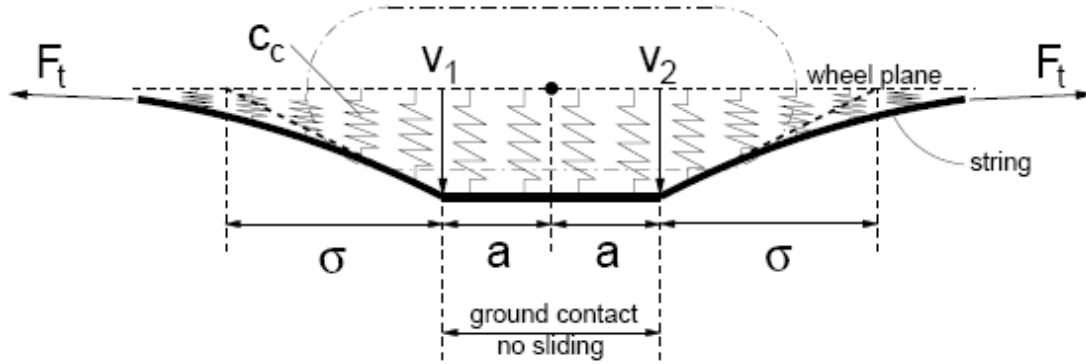
3.8.1 Relaxation Length

Figure- 4 Relaxation and contact patch [22]

Figure- 4 shows a stretched string model from Besselink [22] where the length of the contact patch is represented as 2a. If a low slip angle is applied to a rolling wheel, the wheel continues rolling straight on a constant heading and no appreciable skidding occurs. Then, based on the work of Smiley [19], the tyre builds up a lateral force which exponentially approaches an end-point condition for steady yawed rolling as the tyre tread material enters the contact patch. When a lateral force is applied to a rolling wheel, the upper section of the wheel is considered as a non-deformable element. As it rolls into the bottom section, due to the deformation which already exists in the contact patch, the tyre starts to distort just before it enters the contact patch (i.e. when the tyre material is not yet in contact with the road). A similar phenomenon occurs when the tyre material is exiting the contact patch and a small distance is required for the tyre to recover its original shape. The distance required for the tyre to deform and recover its shape as the tyre rolls into (or out of) the contact patch is called the relaxation length σ and can be calculated using the following conditional equation [19]:

$$
\begin{cases}
\sigma = (11\delta_0/d)\big(2.8 - (0.8p/p_r)\big) & (\delta_0/d \leq 0.053) \\
\sigma = \big[(64\delta_0/d) - 500(\delta_0/d)^2 - 1.4045\big]\big(2.8 - (0.8p/p_r)\big) & (0.053 \leq \delta_0/d \leq 0.068) \\
\sigma = [0.9075 - (4\delta_0/d)]\big(2.8 - (0.8p/p_r)\big) & (\delta_0/d \geq 0.068)
\end{cases} \qquad (13)
$$

2.8.2 Lateral Distortion Estimation

The lateral distortion due to camber angle can be calculated using the camber angle and the vertical deflection of the tyre. For a tyre with a given slip angle, the velocity acting at the wheel centre and in the contact patch are illustrated in Figure-5:
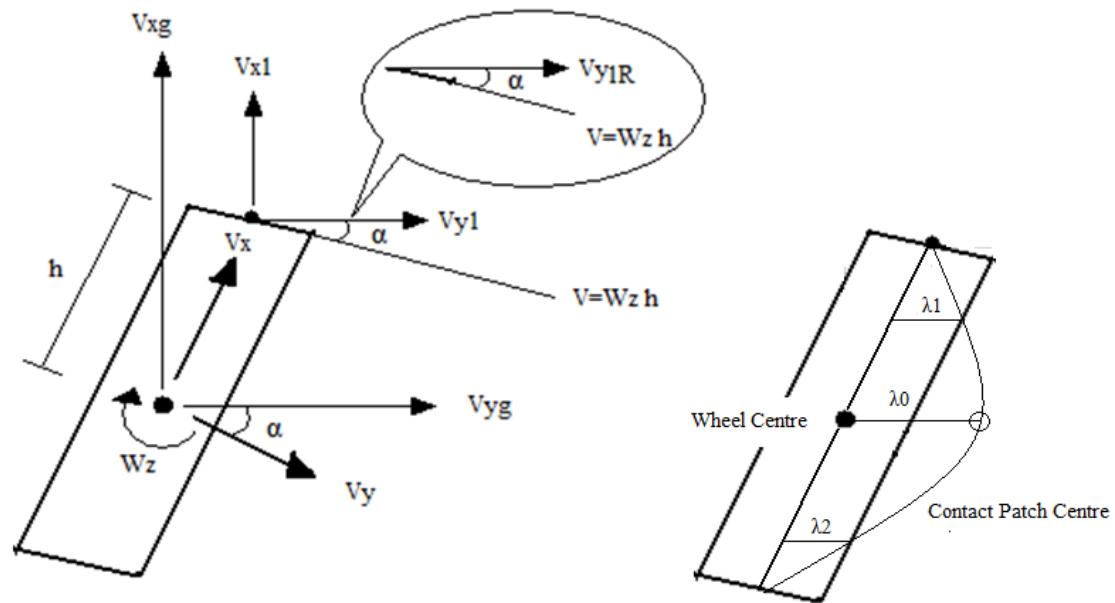

Figure- 5 Tyre Contact Patch

The forward and lateral velocity components at the tyre contact patch centre are given by V_x and V_y. V_{x1} and V_{y1} are the forward and lateral velocity components at the front of the contact patch. V_{xg} and V_{yg} are the forward and lateral velocity components at the wheel centre. The velocity at the front of the contact patch can be calculated as:

$$V_{x1} = V_x/\cos \Psi \tag{14}$$

$$V_{y1} = V_{yg} + V_{y1R} \tag{15}$$

$$V_{yg} = V_y/\cos \Psi \tag{16}$$

$$V_{y1R} = \frac{W_z h}{\cos \Psi} \tag{17}$$

Equation 17 can be written as:

$$V_{y1} = V_{yg} + \left(\frac{W_z h}{\cos \Psi}\right) \tag{18}$$

15

The lateral distortion at the front of the contact patch can be calculated using the following equation:

$$\lambda_1 = \sigma \Psi - \sigma\left(V_{y1}/V_{x1}\right) \tag{19}$$

For a time dependant solution the current solution step should include the same effect as the previous step. If K is assumed to be the current step and T the time of the simulation and a simulation is run, for example, for 10 seconds with 100 steps (when K is 1), the time of a simulation should be at least 0.1s. Also if J is the previous step then it can be seen that $J = K - 1$.

For look back distance:

$$delt0 = \sigma/V_x \tag{20}$$

$$Tback = Time - Time(J) \tag{21}$$

If Tback is greater than delt0:

$$Grad0 = [\lambda_1(K) - \lambda_1(J)]/[Time(K) - Time(J)] \tag{22}$$

$$\lambda_0 = \lambda_1(K) + Grad0 * (Tback - delt0) \tag{23}$$

If $K = 1$ and Tback is smaller than delt0, then

$$\lambda_0 = \lambda_1 \tag{24}$$

For a look back distance H:

$$delt2 = 2\sigma/V_x \tag{25}$$

If Tback is greater than delt2:

$$Grad2 = [\lambda_1(K) - \lambda_1(J)]/[Time(K) - Time(J)] \tag{26}$$

$$\lambda_2 = \lambda_1(K) + Grad2 * (Tback - delt0) \tag{27}$$

16

If K = 1 and Tback is smaller than delt2, then

$$\lambda_0 = \lambda_2 \qquad\qquad (28)$$

In summary the parameters for the new aircraft tyre model are listed in Table- 2:

Table- 2

A1	Tyre pressure coefficient for vertical force calculation
A2	Rated tyre pressure coefficient for vertical force calculation
B1	Rated tyre pressure coefficient for cornering power calculation
B2,B3	Cornering power coefficient for τ below 0.0875
B4,B5	Cornering power coefficient for τ above 0.0875
C1, C2	Yaw angle parameter friction coefficient
D1	Lateral force coefficient for linear deformation phase
E1	Aligning moment coefficient for linear deformation phase
E2	Aligning moment coefficient for transition phase
E3	Aligning moment coefficient for slipping phase

Table- 2 Table of Coefficient Description

4. Co-simulation and Building a Tyre Subroutine in Matlab

The MSC.ADAMS software is a general purpose industry standard multi-body simulation tool where programming tyre model equations directly into ADAMS is based on a code compiling format. This is not always a convenient method for tyre model development if the tyre model needs to be exported to other simulation environments. Developing a tyre subroutine is an effective solution to counter this problem where the tyre subroutine file (.dll) contains all of the constant values, equations and the necessary variables for calculating the tyre model outputs [23]. During simulation information such as slip angel and camber angle is passed to the model subroutine file simultaneously so that it can calculate the tyre force and moment outputs for the next time step and pass these back to the vehicle or aircraft model. The software chosen for the tyre subroutine development for this investigation was Matlab/Simulink®. The process of co-simulation is illustrated in Figure- 6.
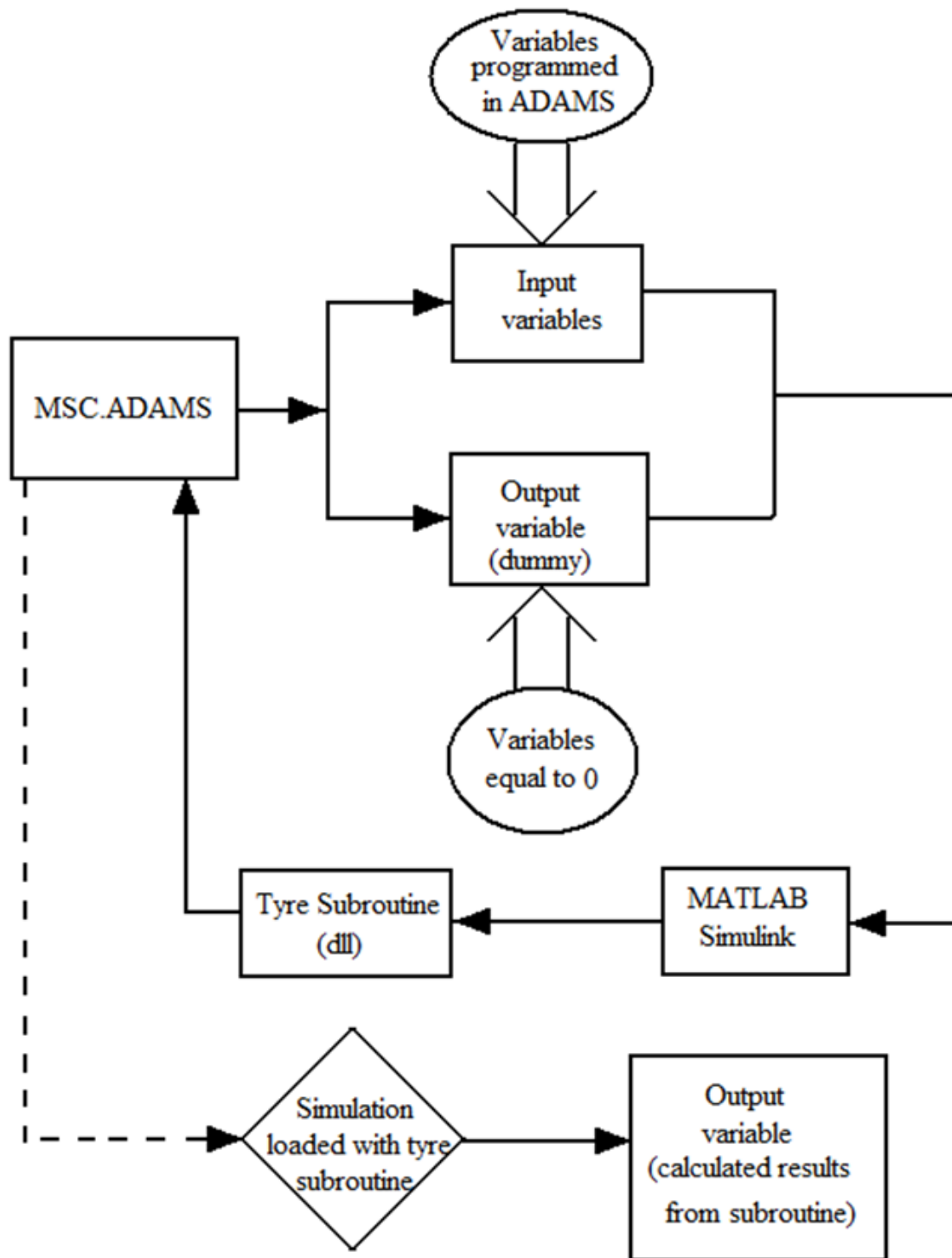
Figure- 6 Import and export variable for Co-simulation

Before developing the tyre subroutine using Matlab/Simulink®, there were a number of preliminary steps. Two sets of state variables were required in order to develop the tyre subroutine. The first set includes the programmed variables calculated by ADAMS such as, longitudinal velocity, lateral velocity and vertical load. These are called 'Input variables' as shown in Figure- 6. The second set of state

variables are dummy variables, i.e. variables set equal to zero. These dummy variables need to be setup in relation to the desire outputs calculated by the tyre subroutine such as longitudinal force, lateral force and aligning moment. After setting the 'control plan export', ADAMS will generate a file that is compatible with Matlab®. Matlab/Simulink®. Unlike other software, instead of using direct programming, Matlab/Simulink® uses block and flow diagrams to represent mathematical calculations.

After the programme in Matlab/Simulink® was completed, the 'real time workshop' function was used to create a subroutine file (.dll) as shown in Figure- 6. The tyre model subroutine was then imported back and integrated with the chosen multi-body simulation model file. Further information on how to setup the 'real time workshop' can be found in [24].

5. Tyre Modelling and Simulation

The tyre model study was initially based on a functional model of the Flat Bed Tyre Test machine from Coventry University [18] as shown in Figure- 7. The tyre rig model contains a number of parts which move forward on a flat uniform road surface in the same way that the tyre interacts with a moving belt on a tyre test machine. The tyre data used for this simulation was based on 'Goodyear' aircraft tyre test data [25]. The simulation recreated tyre tests at four different vertical load cases, and the wheel maintained a constant longitudinal velocity for the entire simulation. For each load case, the tyre performed a positive and negative slip angle sweep at a maximum value of nine degrees. The tyre was then returned to the straight ahead position to continue to the next load case following a process described in [26].
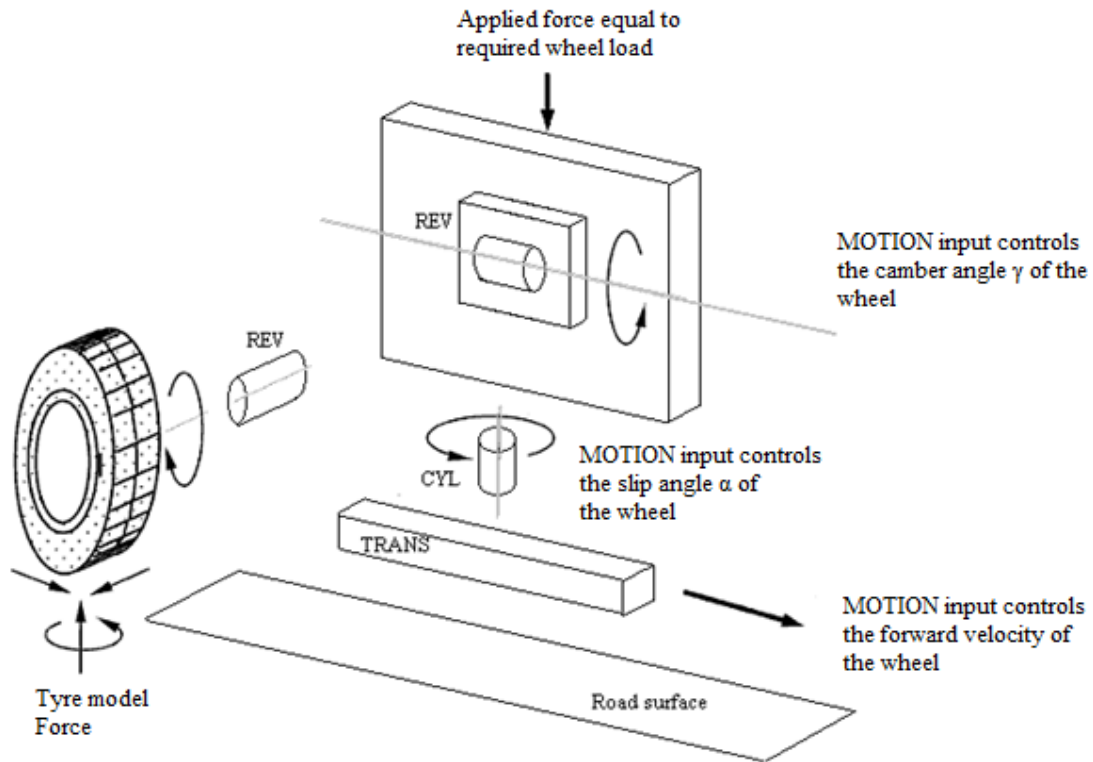
Figure- 7 Test Rig Model [18]

6. Simulated Test Rig Results

Figure- 8 shows the simulation results for slip angle versus lateral force at various tyre loads. For loads corresponding to 4G, 6G and 8G the lateral force increases linearly as the slip angle is varied between plus and minus nine degrees. This shows that the tyre is undergoes elastic deformation in this region. From the 2G test, the lateral force first varies linearly as the slip angle increases. As the slip angle increases beyond six degrees, the lateral force stops increasing and becomes constant. This effect shows that the energy generated from slip angle has passed beyond that which the tyre can sustain which results in the tyre slipping. The slip angle at which the tyre transfers from an elastic deformation state to a slipping state is also known as the critical slip angle. By plotting all four load cases on the same graph, it can be seen that the vertical force does not only influence the lateral force but also the critical slip angle (the point of maximum lateral force). Therefore at higher vertical loads, the tyre will experience a larger range for the elastic deformation state.

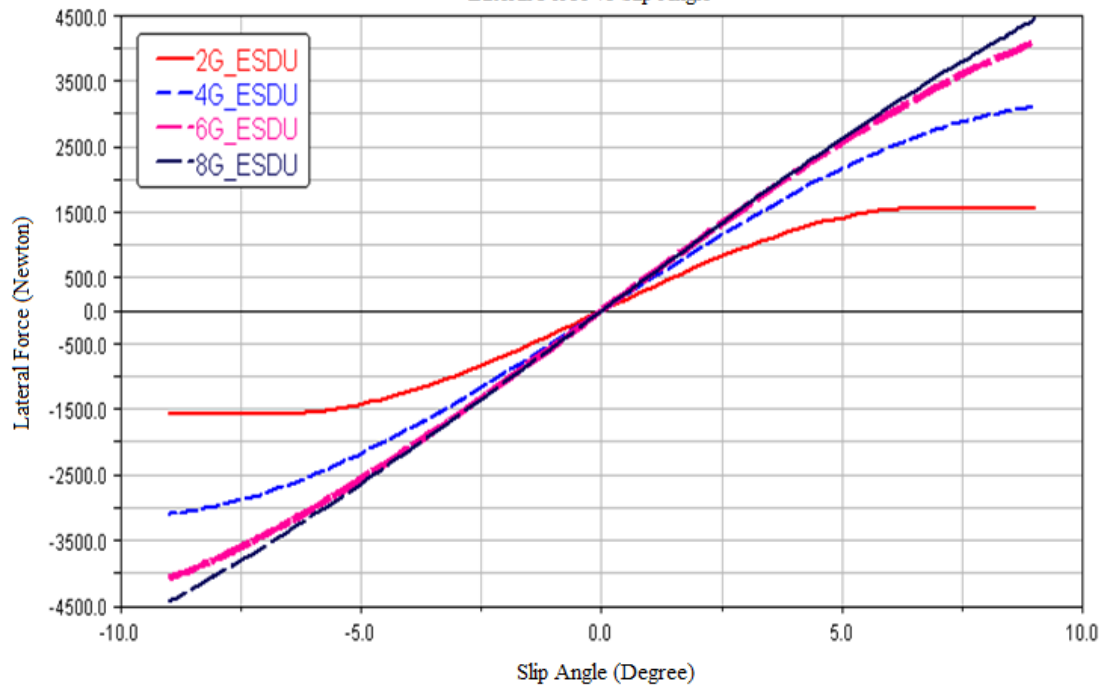**COVENTRY UNIVERSITY TYRE TEST MACHINE**
Lateral Force vs Slip Angle

Figure- 8 Lateral Force versus Slip Angle from Simulation

Figure- 9 shows the aligning moment results. In the elastic deformation state the aligning moment first increases to a maximum value and then decreases to zero as during the slipping phase. In reality it is possible to generate negative aligning moment at low load and high slip angle, however the magnitude is very small and is assumed here to be zero.

Figure- 9 Aligning Moment versus Slip Angle from Simulation

Figure- 10 shows the simulation results for the pneumatic trial. All four load cases show that when the slip angle is zero, the pneumatic trail is at its maximum. In other words, when the wheel is travelling straight on, the resultant vertical force and thus contact patch centre will have its largest longitudinal separation. It can also be seen that as the slip angle increases, the pneumatic trail decreases. When the slip angle reaches the critical slip angle, the pneumatic trial is equal to zero. It is possible to get a negative pneumatic trail if the slip angle increases beyond the critical slip angle. However, the value is relatively small is being assumed to be zero.
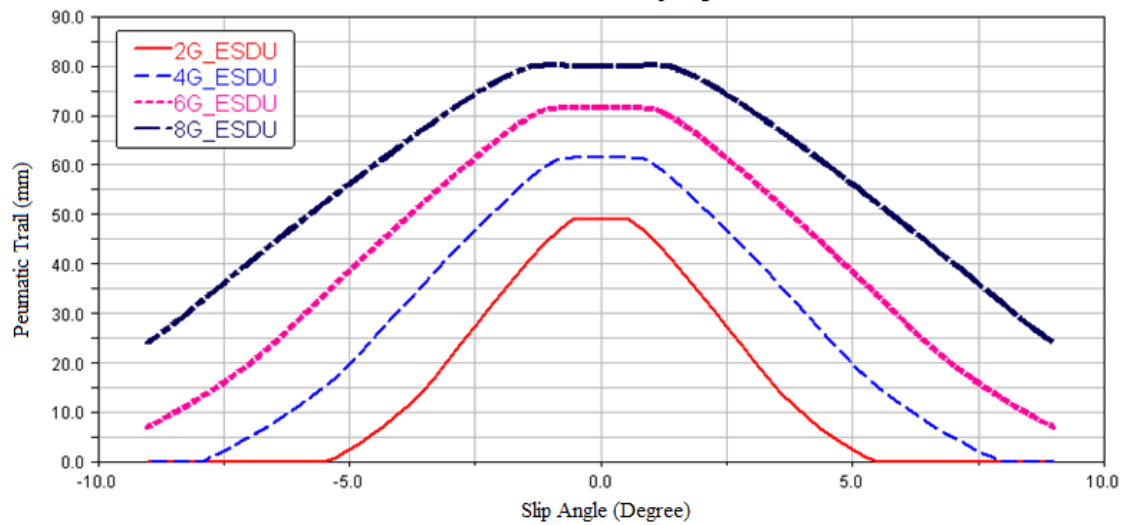
Figure- 10 Pneumatic Trail versus Slip Angle from Simulation

7. Taxiing Manoeuvre with a Full Helicopter Model

Landing gears have an important function to support the aircraft on the ground and to allow it to perform a taxi, take-off or landing manoeuvre [14]. In this study the tyre model was integrated into a full helicopter model to perform taxiing manoeuvre simulations. The helicopter model travelled at a constant taxi velocity (5.14m/s) and performed eight turns, four 45 degree turns (two positive and two negative) and four 90 degrees turns. Figures 11, 12 and 13 show the results extracted from the tyre subroutine.
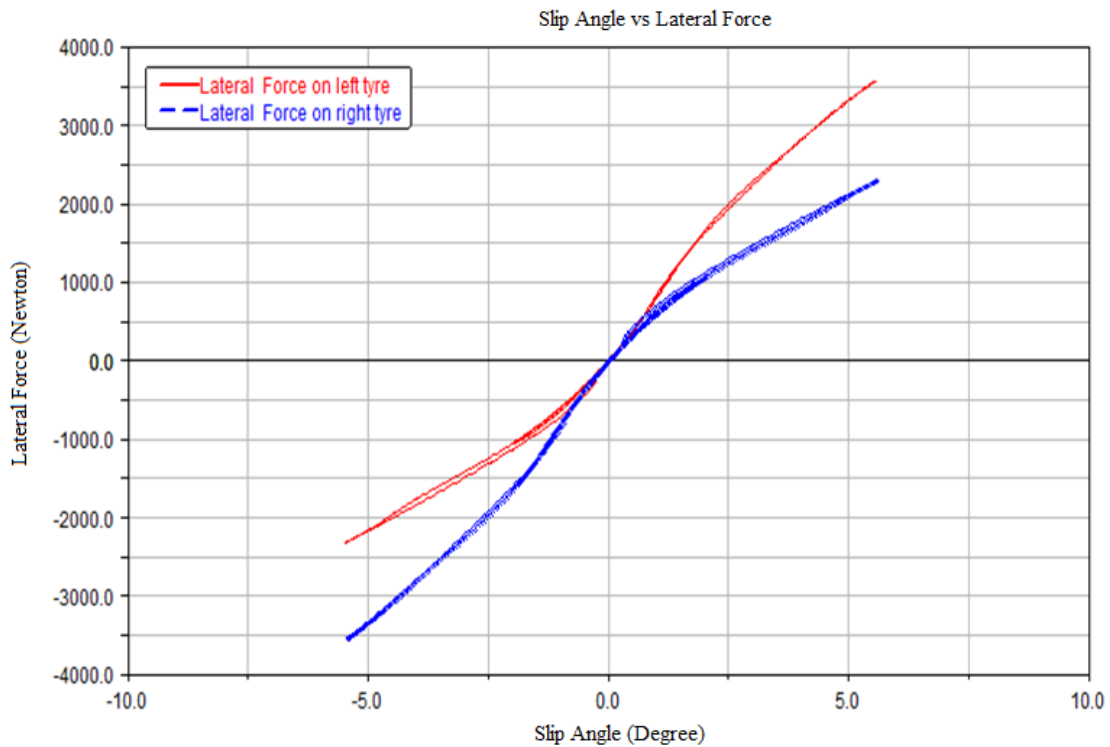
Figure- 11 Slip Angle versus Lateral Force

Figure- 11 shows the lateral force results on both the left and right tyres for the nose landing gear. It can be seen that even though the helicopter has turned to 90 degrees, the slip angle generated in the tyre is only six degrees. The lateral force is still in the elastic deformation state even with the wheels turned at 90 degrees. The nose landing gear has a twin wheel layout; therefore the tyres are not aligned with the centre of mass position. When a lateral force is applied to the tail of the helicopter, it causes weight transfer. This leads to a variation in the vertical force acting at the left and right wheel. The difference in vertical force results in different lateral forces being generated on the left and right tyres. Also, as the slip angle increases from zero to six degrees, it can be seen that the lateral force did not increase nor decrease on a straight line path as shown with the test rig results, but instead followed a looped path. When the helicopter was turning, the lateral force pushed the centre of mass to one side. Therefore more vertical force was generated on one side and resulted in a higher lateral force. When the helicopter was returning to the straight line position, the mass centre shifted to the opposite side and resulted in less vertical force and less lateral force. It is this vertical force variation that causes different results in the lateral force plot while the helicopter performs a taxi manoeuvre.
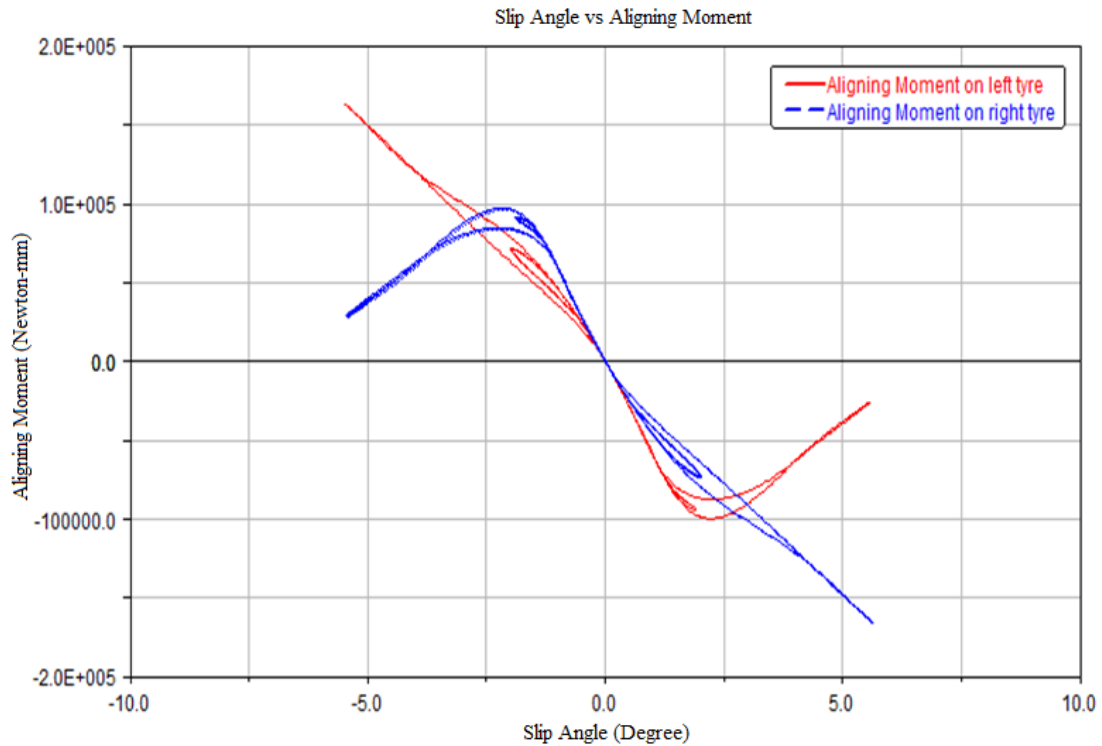
Figure- 12 Slip Angle versus Aligning Moment

Figure- 12 shows the aligning moment results on the left and right tyres. Similarly to the lateral force simulation results, the loop effect can also be seen in the aligning moment results. Both the left and right tyres show the aligning moment has a linear relationship between 0 and ±2.3 degrees of slip angle. As the slip angle increases beyond ±2.3 degrees; the aligning moment behaviour varies depending on the vertical force. Using the positive slip angle results as an example, the right tyre vertical force is higher compared with the left tyre. The results show that the aligning moment continues increasing. Therefore the tyre remains in an elastic deformation state. Due to a lower vertical force acting on the left tyre, the aligning moment decreases as the slip angle is increased beyond ±2.3 degree. If there is any further increase in slip angle, the aligning moment will become zero and the tyre will enter its slipping phase.

In Figure- 13 the graph shows the simulation results on the left tyre plotted as vertical force and aligning moment together against time. It can be observed that for the first six turns, the aligning moment increases and decreases with vertical force. As the helicopter performs its seventh turn, the vertical force decreases from 13000N to 4800N. The aligning moment increases from zero to a negative peak value. Between

175 and 185 seconds, the vertical force becomes stationary and during this time the landing gear is turning towards the 90 degree position. The aligning moment decreases to a positive peak value. As the landing gear turns back, the aligning moment starts to return to a second negative peak. As the vertical force starts to change from constant to a higher value, the aligning moment decreases from the second negative peak value linearly as the vertical force eventually become zero and the tyre returns to its straight line position.
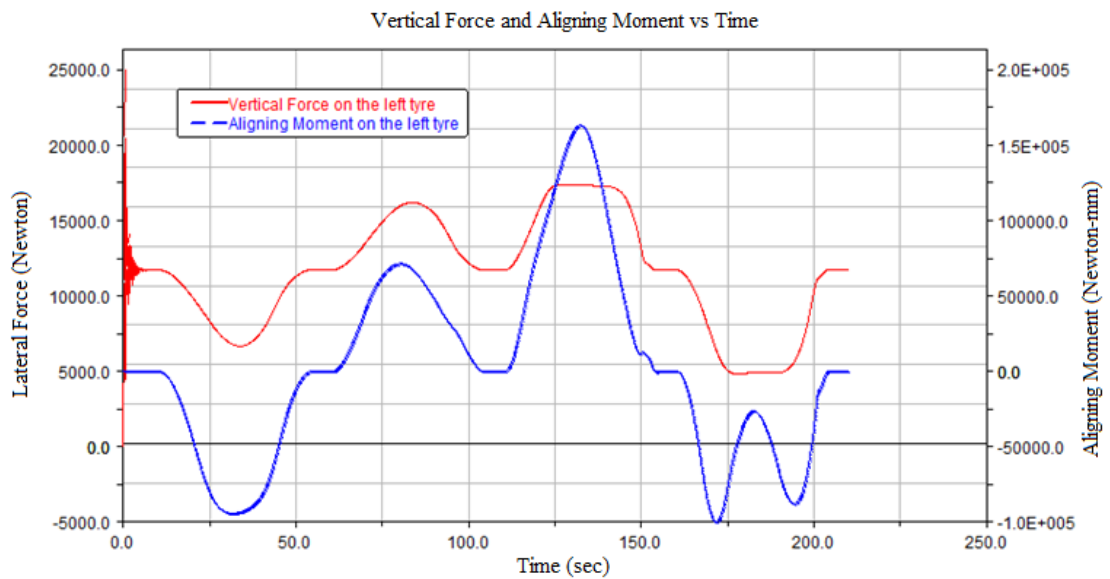

Figure- 13 Time versus Vertical Force and Aligning Moment

8. Conclusions

A unique tyre model was developed specially for helicopter ground operation simulations. Various tyre models were reviewed to provide a basis for the formulations in the new tyre model. Following consideration of existing available tyre models and the with the project research aim of developing a low parameter tyre model, the ESDU tyre model developed by Mitchell [2] was used as the model foundation. The model was completed by adopting other equations from Blundell and Harty [18] and the R-64 model by Smiley [1] resulting in a new model that only requires twenty three input parameters. To make the model portable, a co-simulation method was also utilised. The tyre model was programmed in Matlab/Simulink® and formatted into a subroutine file. The subroutine file was then imported into MSC.ADAMS and loaded with the multi-body helicopter model to perform different simulations. The model was first imported to a virtual tyre test rig to validate the basic properties of the tyre model. The tyre model was then imported to a full helicopter model and used successfully to perform taxiing manoeuvre simulations. From the runway manoeuvre simulation results, the tyre model showed its capability to capture various dynamic characteristics.

The tyre model developed in this investigation has been shown to integrate the low parameter principle whilst maintaining detailed calculations for some of the important tyre responses. The lateral force and the aligning moment were created with a suitable level of precision. However, the aim of this project was to replicate the response of the lateral and longitudinal force of the tyre. This could not be achieved due to a lack of suitable test data. If tyre test data were to become available the tyre model could be developed further. This would significantly advance the research already conducted and lead to improved tools for helicopter design and the simulation of aircraft ground dynamics.

9. References

1. **Smiley, R.F. and Horne, W.B.** Mechanical properties of pneumatic tyres with special reference to modern aircraft tyre R-64, *NASA*,. 1957 (USA)

2. **Mitchell, D.J.** Frictional and Retarding Forces on Aircraft Tyres Part IV: Estimation of Effects of Yaw, *ESDU*,. 1986. **86016**

3. **Pacejka, H.B.** *Tyre and Vehicle Dynamics.* 2006, 321-358 (ELSEVIER, Netherlands, second edition).

4. **Besselink, I.J.M., Schmeitz, A.J.C.,** and **Pacejka, H.B.** *An Improved Magic Formula/SWIFT Tyre Model That Can Handle Inflation Pressure Changes.* 2000, (Department of Mechanical Engineering, Eindhoven University of Technology).

5. **Kiebre, R.** Contribution to the Modelling of Aircraft Tyre-Road Interaction. *University De Haute-Alsace PhD thesis*,. 2010. (France)

6. **Mavros, G., Rahnejat, H. and King, P.D.** Transient analysis of tyre friction generation using a brush model with interconnected viscoelastic bristles. *J. Multibody Dynamics*,. 2004, **219**(K).

7. **Gim, G. and Nikravesh, P. E**. An analytical model of pneumatic tyres for vehicle denamic simulations. *Part 1: pure slips, International Journal of Vehicle Design*,. 1990, **11**(6).

8. **Gim, G. and Nikravesh, P. E**. An analytical model of pneumatic tyres for vehicle denamic simulations. *Part 2: pure slips, International Journal of Vehicle Design*, 1991, **12**(1).

9. **Gim, G. and Nikravesh, P. E**. An analytical model of pneumatic tyres for vehicle denamic simulations. *Part 3: pure slips, International Journal of Vehicle Design*, 1991, **12**(2).

10. **Wood, G.** Aircraft Tyre Modelling. *Coventry University PhD thesis*.. 2006. (U.K.)

11. **Gipser, M.** FTire - Flexible Ring Tire Model. *Cosin Scientific Software*,. 2013.

12. **YANG, X.G.** Finite Element Analysis and Experimental Investigation of Tyre Characteristics for Developing Strain-based Intelligent Tyre. *Birmingham University PhD thesis*,. 2011. (U.K.)

13. **Moreland, W.J.** The Story of Shimmy. *Journal of the Aeronautical Sciences*,. 1954. **21**(12).

14. **Moore, D.F.** *The Friction of Pneumatic Tyres.* 1975, 323-325 (ELSEVIER, Amsterdam-Oxford-New York).

15. **Grossman, D.T.** F-15 nose landing gear shimmy, taxi test and correlative analyses. *SAE Technical Paper,*. 1980, **801239**

16. **Haney, P.** *The Racing and high-performance tyre*, 2003, (TV MOTORSPORTS and SAE, United States of America) **R-351**.

17. **Butts, D. and Kogan, A.** Helicopter landing gear shimmy analysis. *American helicopter society international, Inc,*. May 2010. (66th Annual Forum, Phoenix, AZ, USA)

18. **Blundell, M.V. and Harty, D.** *The Multibody systems Approach to Vehicle Dynamics.* 2004, 248~325 (ELSEVIER, UK).

19. **Smiley, R.F.** Correlation, Evaluation, and Extension of linearized theories for tyre motion and wheel shimmy. *NASA,*. 1956.

20. **Balkwill, K.J.** Comprehensive method for modeling performance of aircraft type tyres rolling or braking on runways contaminated with water, slush, snow, ice. *ESDU,*. May 2005. **05011.**

21. **Page, A.N.** Frictional and Retarding Forces on Aircraft Tyres Part IV: Estimation of Effects of Yaw. *ESDU,*. 1986, **71025**.

22. **Besselink, I.J.M.** Shimmy of aircraft main landing gear. *voorzitter van het College PhD thesis,*. 2000. (Netherlands)

23. **Feng, J.Z., Yu, F. and Zhao, Y.X.** Design of a Bandwidth-limited Active suspension Controller for Off-Road Vehicle Base on the Co-simulation Technology. *Journal of Shanghai Jiao Tong University,*. 2004, **3**(1).

24. **MSC.ADAMS,** Getting Started Using ADAMS/Controls. *MSC.Software Corporation*, year 2004.

25. **Aircraft tyre engineering GOODYEAR tyre and rubber company.** Nosewheel tyres for the Westland Helicopter. *Agusta Westland Helicopter*, March 1989.

26. **HEGAZY, S., H. RAHNEJAT**, and **K. HUSSAIN**. Dynamic tyre testing for vehicle handling studies. *Multibody Dynamics: Monitoring and Simulation Techniques II,*. 2000, **135.**

List of Figures